

Bluetooth clones for communication reliability

X. Xiong and J.K. Pollard

Abstract

Bluetooth-enabled sensors may be used for monitoring personal health but there is considerable distortion of the received signal. A new topology of Bluetooth radio system using cloned devices is presented. The distortion at the receiver was reduced in order to achieve low Bit Error Rate (BER). Computer modelling was conducted for testing this innovation.

1. Introduction

Communication reliability is very important for sets of wireless-enabled sensors that monitor the health of people in their home. Personal safety may be at stake.

A suitable technology is a Bluetooth Personal Area Network (PAN). This is a set of low power, inexpensive, short-range (10-100m) radio transceivers that operate at 2.45 GHz [1]. A single Master controls no more than seven Slaves in a Piconet and a PAN comprises several communicating Piconets.

Packets of information are transmitted over radio channels that suffer co-channel interference. This is due to multiple paths between source and sink because of the many irregular scatterers (walls or furniture) in an indoor environment. Many errors appear at the receiver.

The aim of the present work is to reduce the communication errors by adding redundancy in connectivity for the channel. Bluetooth *clones*¹ allow two links between Master (+ Master-Clone) and Slave.

Computer modelling has been used to confirm the observed performance of a single Bluetooth radio link [2]. This work is extended to examine the cloned communication system and to determine its improvement in terms of Bit Error Rate.

2. Clone topology

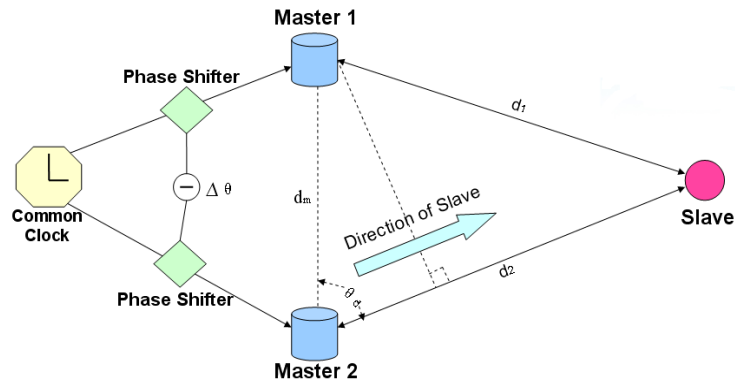


Figure 1 Schematic diagram of cloned Bluetooth system

The topology of a cloned Bluetooth system is presented in Figure 1. Master1 and Master2 (Master-Clone) are synchronized by a common clock and communicate with a Slave. Phase shifters are used in order to set different delays of the transmitted signals at the Master end.

The idea of this design is to reduce the affect of reflection in fading channel. In this topology, the original signal is transmitted by two identical Masters and reach to the Slaves with varied phase shift. As the two signals meet with different reflections while passing through the indoor channels, they would not suffer the largest fading at the same time. After being received and added at the Slave, the quality of the received signal will be improved since the signals from different channels compensate each other so as to reduce the interference from the scatterers.

3. Modelling process

3.1 Overview

For verifying above proposal, we examine the characteristics of baseband signal throughout the entire transmission process by using computer modelling. A general model is illustrated in Figure 2.

¹ A cloned Bluetooth device has an independent clock but has a common address and memory.

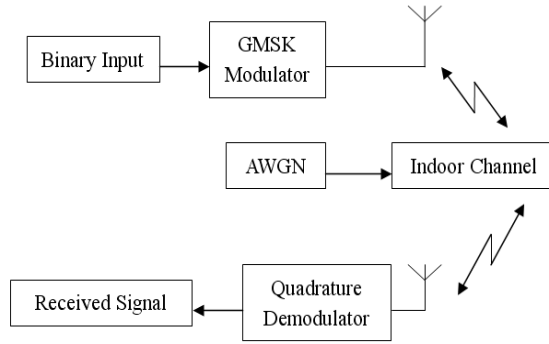


Figure 2 General communication model

Maximal length shift-register binary data are up-converted by a Gaussian Minimum-Shift-Key (GMSK) Modulator at a prescribed carrier frequency. The passband signal then passes through the multipath indoor channel with Added White Gaussian Noise (AWGN). At the receiver end, a quadrature demodulator is adopted to recover the original baseband signal.

3. 2 Modulation

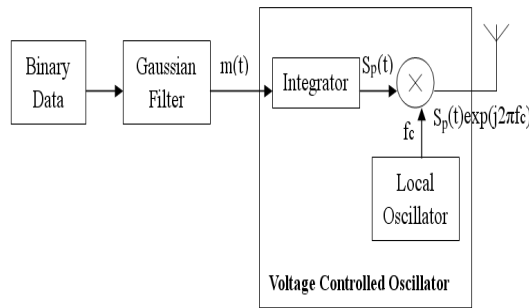


Figure 3 GMSK Modulator

Figure 4 shows a simulation model of GMSK modulator. A Gaussian filter shapes sampled binary data. Samples are fed to Voltage Controlled Oscillator (VCO) where they are integrated and up converted to high frequency band.

The two signals $s_1(t)$ and $s_2(t)$ transmitted from two Masters which are subject to different phase delay could be expressed as $\text{Re}[\hat{S}(t)\exp(j2\pi fct + \phi_1)]$ and $\text{Re}[\hat{S}(t)\exp(j2\pi fct + \phi_2)]$, respectively.

Continuous-Phase Frequency-Shift Keying (CPFSK), is used as the modulation scheme. The passband CPFSK signal, $S_p(t)$ is:

$$S_p(t) = A \cos[\theta(t)] \cos(2\pi fct) - A \sin[\theta(t)] \sin(2\pi fct) = \text{Re}[S_b(t) \exp(j2\pi fct)] \quad \text{Eq. 1}$$

where A is the constant envelope of the modulated signal, f_c is carrier frequency (2.45 GHz). $\text{Re}[\]$ is the real part of the complex number and $S_b(t)$ is the baseband modulated signal:

$$S_b(t) = \cos[\theta(t)] + j \sin[\theta(t)] \quad \text{Eq. 2}$$

Here, $\theta(t)$ is the phase of the signal:

$$\theta(t) = \int m(t) dt \quad \text{Eq. 3}$$

where $m(t)$ is the Gaussian shape sampled binary data signal to be transmitted over the channel [4].

3. 3 Indoor Channel

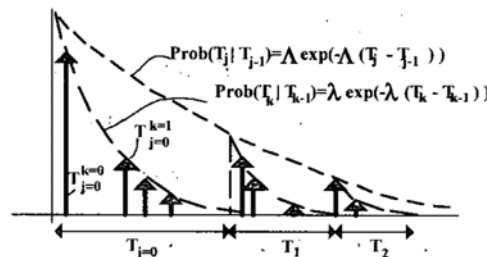


Figure 4 Double-Poisson arrival channel model [3]

Figure 4 shows a statistical model for indoor multipath propagation.[3]. There are three clusters of waves which follow different reflection paths illustrated in this figure. These clusters are several nanoseconds delayed with respect to the Line-of-Sight (LOS) wave.

At this stage, we pass signals $S_{p1}(t)$ and $S_{p2}(t)$ through two example indoor channels which are simulated based on the same model shown in Figure 4. The method is to simulate the two signals propagated over two different channels in indoor environment. Additionally, AWGN samples are generated using the Box-Muller method [5].

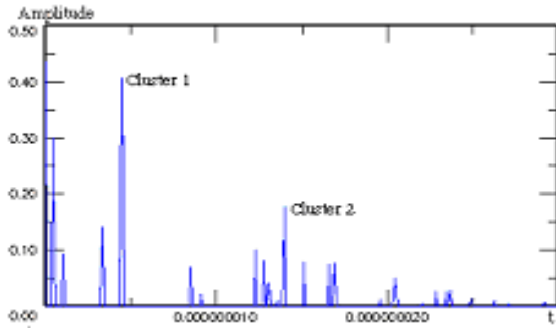


Figure 5 Channel impulse response

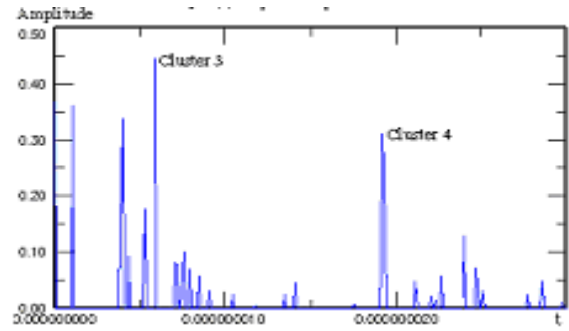


Figure 6 Channel impulse response

Figures 5 and 6 are the impulse response of the two example indoor channels by inputting ideal pulse with unit amplitude for the first sample and zero for others. They show that the clusters in channel 1 were delayed from those of channel 2. This indicates that a large interference would not occur at the same time in the two channels.

3. 4 Demodulation

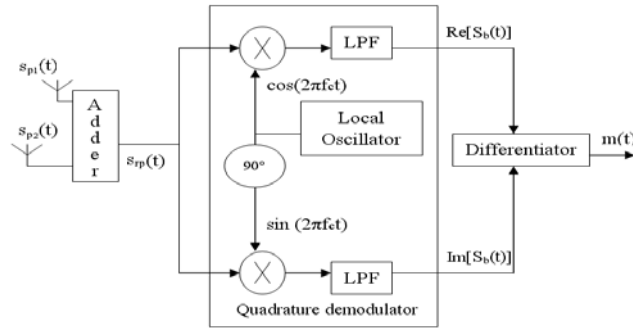


Figure 7 Demodulator model

Figure 7 indicates a demodulator is actually consists of an adder, a quadrature demodulator and a differentiator. The recovered baseband signal $m(t)$ can be used to examine the transmission characteristics.

Quadrature demodulation is employed to down convert the passband signal to baseband. The mathematic demodulation procedures are explained below.

$$\begin{aligned} S_{sp}(t)\cos(2\pi f_c t) &= [A\cos[\theta(t)]\cos(2\pi f_c t) - A\sin[\theta(t)]\sin(2\pi f_c t)]\cos(2\pi f_c t) \\ &= \frac{1}{2}A \cos[\theta(t)][1+\cos(4\pi f_c t)] - \frac{1}{2}A\sin[\theta(t)] \sin(4\pi f_c t) \end{aligned} \quad \text{Eq. 4}$$

$$\begin{aligned} S_{sp}(t)\sin(2\pi f_c t) &= [A\cos[\theta(t)]\cos(2\pi f_c t) - A\sin[\theta(t)]\sin(2\pi f_c t)]\sin(2\pi f_c t) \\ &= \frac{1}{2}A \cos[\theta(t)]\sin(4\pi f_c t) + \frac{1}{2}A\sin[\theta(t)][\cos(4\pi f_c t)-1] \end{aligned} \quad \text{Eq. 5}$$

$$m(t) = \frac{d\theta(t)}{dt} \quad \text{Eq. 6}$$

From Eq.4 and Eq.5, we can see the baseband signal is able to be recovered by multiplying the carrier signal and removing their high frequency component. A differentiation is then required for recovering the Gaussian shape sampled signal in terms of Eq.6

4. Modelling result

The result that had similar format to that in was obtained after conducting above simulation procedure.

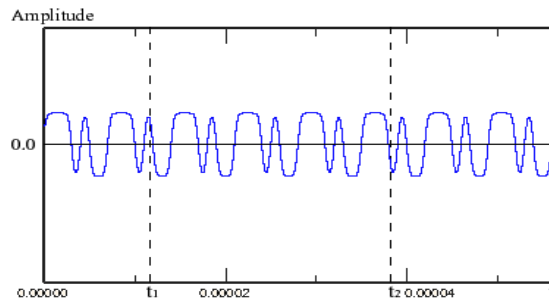


Figure 8 Original data after Gaussian filter

Figure 8 is data filtered by Gaussian filter.

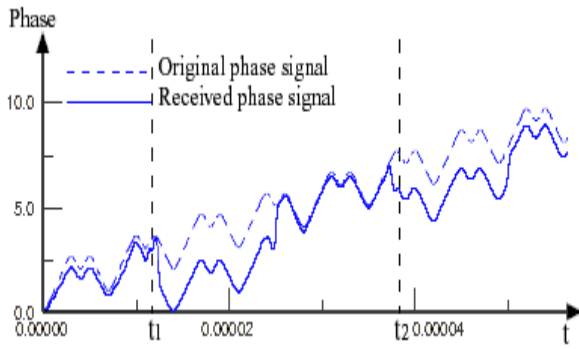


Figure 9 Phase vs time for original data

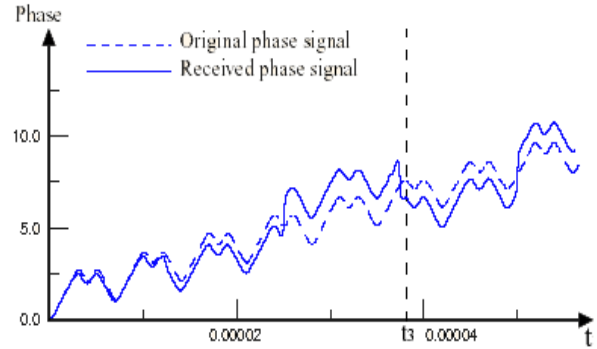


Figure 10 Phase vs time for cloned data

In Figure 9, the broken line represents the phase signal integrated from the original signal. The continuous line is the phase signal after being passed through the indoor channel. Distortion can be seen. This is due to reflected waves and causes errors in received data.

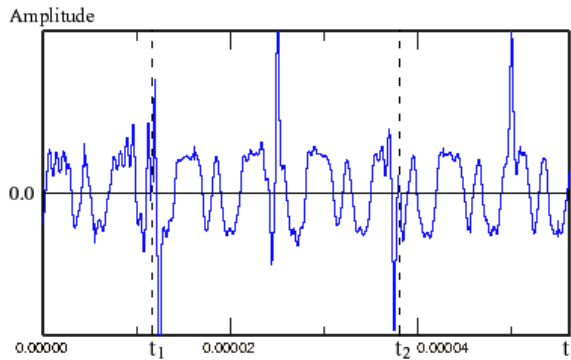


Figure 11 Recovered signal for original data

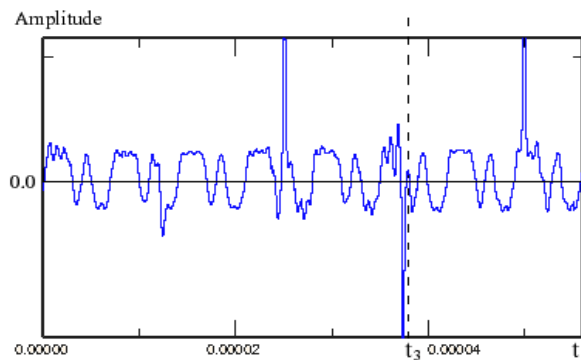


Figure 12 Recovered signal for cloned data

The original and received phase signal for a single set of data are shown in Figure 9. Figure 10 and Figure 11 show the received phase signal and recovered Gaussian filtered sampled signal with $\pi/4$ and $-\pi/4$ phase shift between two arrival signals, respectively.

The wave form of the signal in Figure 10 is smoother and less severe distortion points occur in certain time period than for Figure 9. This signal is more approximate to original phase signal. The quality of the recovered Gaussian filtered sampled signal should be better than in one Master case as it is recovered by differentiating the signal in Figure 10. We can see from Figure 12 that only one error is produced in detection at time t_3 within the same measurement period as in Figure 9. It could be inferred that lower BER can be achieved under the cloned Master topology.

Consequently, we can claim here the novel topology is able to reduce the affect of reflection in multipath and fast fading channel and enhance the performance of transmission. Modelling and measurements are continuing.

5. Summary

The innovative *cloned*-Masters topology was proposed and has been simulated over the realistic model of Bluetooth radio system. The characteristics of baseband signal were examined. The initial theory of this topology was verified to be feasible and useful as the better signal quality was capable of being achieved. The hardware measurement could then be implemented based on the results in this report.

6. Reference

- [1] "Specifications of the Bluetooth System. V1.2" , <http://www.bluetooth.com>, (Nov., 2003).
- [2] J.K. Pollard and N.P. Kontakos, "Bluetooth Indoor Channel Simulation", IEEE Intelligent Data Acquisition & Advanced Computing Systems, Lviv, Ukraine, (Sept., 2003), pp 39-42.
- [3] A.A.M. Saleh and R.A. Valenzuela, "A Statistical Model for Indoor Multipath Propagation", IEEE J. Sel. Areas Coms, VOL. SAC-5(2), (Feb., 1987), pp 128-137.
- [4] S. Haykin, "Communication Systems", Wiley, 2000.
- [5] W.H. Press, et al.. "Numerical Recipes in C", Cambridge University Press, 1988.
- [6] G. Brabant, "Bluetooth in Space", Final project report for Msc. in Spacecraft Technology and Satellite Communications, University College London, (July, 2003)